Fingerprinting of skin cells by live cell Raman spectroscopy reveals melanoma cell heterogeneity and cell-type specific responses to UVR

Emma L. Wilkinson[1], Lorna Ashton[2], Jemma G. Kerns[3], Sarah L. Allinson[1] and Richard L. Mort[1].

1. Division of Biomedical and Life Sciences, Faculty of Health and Medicine, Lancaster University, Bailrigg, Furness Building, Lancaster LA1 4YG, UK.
2. Department of Chemistry, Lancaster University, Lancaster, LA1 4YG, UK
3. Lancaster Medical School, Faculty of Health and Medicine, Lancaster University, Lancaster, LA1 4YG, UK.

ABSTRACT:

Raman spectroscopy is an emerging dermatological technique with the potential to discriminate biochemically between cell types in a label free and non-invasive manner. Here we use live single cell Raman spectroscopy and principal component analysis (PCA) to fingerprint mouse melanoblasts, melanocytes, keratinocytes and melanoma cells. We show the differences in their spectra are attributable to biomarkers in the melanin biosynthesis pathway and that melanoma cells are a heterogeneous population that sit on a trajectory between undifferentiated melanoblasts and differentiated melanocytes. We demonstrate the utility of Raman spectroscopy as a highly sensitive tool to probe the melanin biosynthesis pathway and its immediate response to UV irradiation revealing previously undescribed opposing responses to UVA and UVB irradiation in melanocytes. Finally, we identify melanocyte specific accumulation of β-carotene correlated with a stabilisation of the UVR response in lipids and proteins consistent with a β-carotene mediated photoprotective mechanism. In summary our data show that Raman spectroscopy can be used to determine the differentiation status of cells of the melanocyte lineage and describe the immediate and temporal biochemical changes associated with UV exposure which differ depending on cell type, differentiation status and competence to synthesise melanin.

INTRODUCTION:

Melanocytes are the pigment-producing cells found in the skin, hair and eyes. Melanoblasts are the embryonic precursors of melanocytes and are derived from a transient tissue known as the neural crest (Mort, Jackson and Elizabeth Patton, 2015). Melanoma, the cancer of melanocytes, is the deadliest form of skin cancer with a rising worldwide incidence (Linos *et al.*, 2009; Erdei and Torres, 2010). The risk of developing melanoma is increased by exposure to ultraviolet radiation (UVR) from the sun and from tanning beds (Baldea, Mocan and Cosgarea, 2009; Wallingford *et al.*, 2013).

In human skin, terminally differentiated melanocytes reside in the basal layer of the epidermis (Mort, Jackson and Elizabeth Patton, 2015). Here, melanocytes and keratinocytes are organised into an epidermal melanin unit where a single melanocyte uses its dendrites to makes contact with around 36 keratinocytes (FITZPATRICK and BREATHNACH, 1963; Jimbow *et al.*, 1976). Melanin is manufactured from tyrosine and phenylalanine through a series of enzymatic conversions involving phenylalanine hydroxylase (PAH), tyrosinase (TYR) and dopachrome tautomerase (DCT) (Schallreuter *et al.*, 1994). To protect the skin from the harmful effects of UVR, melanocytes use dendrites to export melanin containing melanosomes to the surrounding keratinocytes which they then arrange above their nuclei to protect them from DNA damage (Kobayashi *et al.*, 1998; Maddodi, Jayanthy and Setaluri, 2012).

Mutations in melanocytes that can cause melanoma arise from DNA damage either caused directly by UVB irradiation or indirectly following UVA irradiation mediated through the generation of reactive oxygen (ROS) species via photosensitiser-mediated processes (Ikehata and Ono, 2011). Solar UVR is composed of mainly UVA (320-400nm wavelengths) with a lesser component of UVB (280-320 nm wavelengths) and a UVA/UVB ratio of about 20

depending on latitude and time of day (Kollias, Ruvolo Jr and Sayre, 2011). Melanocytes respond differently to the UVA and UVB components of solar radiation. UVA irradiation induces immediate pigment darkening through photo-oxidation of melanin that can be observed within minutes of exposure (BACHEM, 1955; Hönigsmann *et al.*, 1986). UVB irradiation on the other hand induces a proliferation in the number of melanocytes in the epidermis (Sato and Kawada, 1972; Rosdahl, 1979; Nordlund, Ackles and Traynor, 1981) as well as activation of melanogenic enzymes in response to DNA photo damage resulting in a delayed tanning response occurring 2-3 days post exposure (BACHEM, 1955). As well as their effects on DNA and on melanin biosynthesis UVA and UVB cause ROS mediated lipid peroxidation (Bose, Agarwal and Chatterjee, 1989, 1990; Filipe *et al.*, 2013), and widespread oxidative modification of proteins resulting in their proteasomal degradation (Grimm, Höhn and Grune, 2012).

Fingerprinting of the biochemical features of individual cell types in the skin and their response to UVR are central to the development of better screening and diagnostic tools in the fight against melanoma. Raman spectroscopy is an emerging technique in cancer research that enables a non-invasive label free analysis of the biochemical structures present within a sample (Brauchle *et al.*, 2014; Moncada *et al.*, 2016). Laser light is used to excite a sample and changes in the scattering that occur through molecular vibrations in proteins, lipids and nucleic acids provide information about the molecular structures present (Gniadecka *et al.*, 2004). Although previous studies have discriminated between normal and melanoma biopsy tissue and between melanocytes and melanoma cells (Silveira *et al.*, 2012; Brauchle *et al.*, 2014) none have examined differentiation status within the melanocyte lineage. This is pertinent because distinct melanocyte populations, of unknown function, reside side-by-side in the interfollicular

epidermis (Glover et al., 2015; Köhler et al., 2017) and melanoma cells are thought to acquire features of embryonic melanoblasts during metastasis (Marie et al., 2020).

Here, we use live single cell Raman spectroscopy and principal component analysis (PCA) to determine whether we could distinguish melanoblasts, melanocytes, keratinocytes and melanoma cells using their biochemical fingerprints. We identify the principal biomolecules that underlie these spectra and examined their response to UVA, UVB and a mixed UVA/UVB light sources. We show that Raman spectroscopy is a highly sensitive method of discriminating between these cell types and probing their responses to UVR.

RESULTS:

Live single-cell Raman spectroscopy can discriminate between skin cell types and melanocyte differentiation status

In order to investigate the cell types in mouse skin with Raman spectroscopy we modelled keratinocytes, melanoblasts, melanocytes and melanoma cells using the COCA, melb-a, melan-a and B16F10 cell lines respectively (Figure 1a) (FIDLER, 1973; Sviderskaya, Wakeling and Bennett, 1995; Diwakar *et al.*, 2008; Segrelles *et al.*, 2011) and used live single cell Raman spectroscopy to acquire individual spectra allowing us to establish their biochemical fingerprints. We confirmed the viability of the cells after imaging using a CellTiter-Glo assay (Supplementary Figure 1a-c) to ensure any observed differences were not attributable to cell death during acquisition. The mean Raman spectra for each cell type (n = 9) appeared qualitatively distinct under normal culture conditions (Figure 1b). In order to further identify the chemical differences, principal component analysis (PCA) was performed, which demonstrated that the main differences between the spectra were accounted for by cell type. As might be expected, we observed tight groupings for the melanoblasts (melb-a), melanocytes

(melan-a) and keratinocytes (COCA) while melanoma cells (B16F10) were more heterogeneous in nature falling between the melanoblast and melanocyte groups on the PCA plot (Figure 1c). The PCA factor loadings (Figure 1d) were used to identify the principal Raman peaks responsible for the PCA groupings and attribute these peaks to their likely biomarkers using the established Raman literature (numbered 1-10 in Figure 1B and summarised in Supplementary Table 1).

Nine of the ten peaks had been previously described and were consistent with the biochemical properties of the cell types examined including melanin biosynthesis (phenylalanine, tyrosine, melanin) photoprotection (β-carotene) or keratinocyte function (keratin/lipid) (Supplementary Table 1). We identified a peak at 1333 cm^{-1} specifically in melanocytes not previously attributed to a known biomarker. As phenylalanine, tyrosine, and melanin peaks were clearly present in these cells we hypothesised this peak might correspond to the melanin precursor DOPA and therefore independently validated the melanin and DOPA peaks using synthetic molecules confirming the presence of a DOPA peak at 1333 cm^{-1} and a melanin peak at 1580 cm^{-1} (Supplementary Figure 1a and b).

As expected, undifferentiated melanoblasts (melb-a) and keratinocytes (COCA) did not exhibit melanin peaks while the pigmented melanocytes (melan-a) and melanoma cells (B16F10) did (Figure 1b). Furthermore, accumulation of phenylalanine was apparent in melanoblasts, keratinocytes and melanoma cells but not in melanocytes presumably because melanin synthesis depletes the phenylalanine precursor in melanocytes. We observed DOPA peaks in melanoblasts (melb-a) and keratinocytes (COCA) both cell types have both been shown to convert tyrosine to DOPA (Schallreuter *et al.*, 1992, 1995; Gillbro *et al.*, 2004). These data demonstrate that live single cell Raman spectroscopy can biochemically discriminate

individual cell types, melanocyte differentiation status and be used to interrogate the melanin synthesis pathway.

Immediate and temporal effects on melanin biosynthesis pathways after UV irradiation detected by Raman spectroscopy

Having established distinct Raman spectra for each cell type we then investigated how they might change in response to UV irradiation. Melanin biosynthesis proceeds through a stepwise conversion of phenylalanine through tyrosine and by the enzymes phenyalanine hydroxylase (PAH), tyrosinase (TYR), dopachrome tautomerase (DCT) and tyrosinase related protein 1 and 2 (TYRP1 and TYRP2) (Cichorek *et al.*, 2013). As demonstrated above, melanocytes (melan-a) and melanoma cells (B16F10) are competent to perform all of these enzymatic steps whilst melanoblasts (melb-a) appear able to synthesise tyrosine but are unable to convert DOPA to melanin (Sviderskaya, Wakeling and Bennett, 1995). Although the enzymatic pathways are well delineated the immediate and short-term biochemical response to UV exposure are still poorly understood. We therefore focused on the melanin biosynthesis pathway immediately after UV exposure by comparing log2 fold change (Log2-FC) in mean Raman peak height (n = 18 spectra in all cases) from control for the biomarkers identified above (Figure 2 and Table 1) in response to irradiation from a UVA, UVB and a mixed UVA/UVB light source over a one to 24-hour response period.

As expected, melanocytes (melan-a) were the most responsive to UVR. We observed a rapid (within one hour) and transient (up to six hours) statistically significant increase in the phenylalanine peak and a rapid (within one hour) and transient (up to six hours) statistically significant decrease in the tyrosine peak after UVA exposure (Figure 2a, Supplementary Figure 3a). In parallel we observed significant reductions in gene expression of *Mitf*, *Dct*, *Tyr* and

Tyrp1 as measured by RT-qPCR at 16 and 24 hours post irradiation (Figure 2d). Together these results suggest a block in melanin synthesis and accumulation of the phenylalanine precursor in the 24 hours post UVA exposure. The changes in melanin levels detected by Raman after UVA irradiation were mirrored by similar trends in intracellular melanin measurement between 0 (control) and 1-3 hours (Figure 2f).

We observed opposing effects on the melanin biosynthesis pathway of UVB compared to UVA in melanocytes (melan-a), as measured by Raman spectroscopy. This was characterised by a statistically significant rapid (within one hour) and sustained (up to 24 hours) decrease in the phenylalanine peak and a rapid (within one hour) and sustained (for up to 24 hours) statistically significant increase in the tyrosine, DOPA and melanin peaks (Figure 2b). Consistent with a rapid UVB response increasing melanin production independent of gene expression, we did not observe any accompanying changes in the gene expression levels of *Mitf*, *Dct*, *Tyr* and *Tyrp1* as measured by RT-qPCR at 16 and 24 hours post irradiation (Figure 2e). The changes in melanin levels detected by Raman after UVB irradiation were mirrored by similar trends in intracellular melanin measurement between 0 (control) and 1-3 hours (Figure 2f).

The response of melanocytes to a mixed UVA/UVB light source appeared more nuanced with features of both the UVA and UVB responses (Figure 2c). However, the UVB response dominated with a rapid (one to three hours) and transient (up to three hours) statistically significant reduction in phenylalanine and a delayed (after one hour) and transient (less than 24 hours) statistically significant increase in the melanin peak. The changes in melanin levels detected by Raman after UVA/UVB irradiation were mirrored by similar trends in intracellular melanin measurement between 0 (control) and 1-3 hours (Figure 2f).

While melanocytes (melan-a) appear to respond differently to UVA vs UVB, melanoma cells (B16F10) demonstrated similar responses to the three light sources. We observed a rapid (within one hour) and sustained (at least 24 hours) statistically significant increase in the phenylalanine peak post UVA irradiation (Figure3a) and a delayed (between six and 24-hours) and sustained (at least 24-hours) statistically significant increase in the phenylalanine peak post UVB and UVA/UVB irradiation (Figure 3b-c). This was accompanied by a statistically significant decrease in the melanin peak between one and 24-hours post UVB and UVA/UVB exposure (Figure 3b-c). The reduction in the melanin peak was the most pronounced after UVB treatment (Figure 3b) and we observed a corresponding reduction in the gene expression of *Tyrp1* at 16 and 24 hours suggesting a block in melanin synthesis (Figure 3e) similar to the one observed in melanocytes (melan-a) after UVA treatment above. The changes in melanin levels detected by Raman after UVA irradiation were mirrored by similar trends in intracellular melanin measurement between 0 (control) and 1-3 hours (Figure 2f).

Consistent with their undifferentiated state we observed a subdued UV response in the melanin biosynthesis pathway in melanoblasts (melb-a). Following UV exposure, we observed a delayed (between 16 and 24 hours) statistically significant reduction in the phenylalanine and the tyrosine peaks (Figure 4a) whilst following UVB exposure we saw an immediate (between 1 and 3 hours) and transient (up to 6 hours) statistically significant reduction in the phenylalanine and tyrosine peaks (Figure 4b). As before, the response to the mixed UVA/UVB light source had features of the UVA and UVB responses with immediate (within one hour) and delayed (by 16-24 hours) statistically significant reductions in the phenylalanine and tyrosine peaks (Figure 4c). Taken with the results from the melanocytes (melan-a) and melanoma (B16F10) cells these results suggest that whilst accumulation of phenylalanine may be due to a block in the melanin biosynthesis pathway, reductions in phenylalanine, detected

by Raman spectroscopy, can occur both through rapid production of melanin depleting the phenylalanine precursor but may also occur independently perhaps through photodegradation as previously reviewed (Kerwin and Remmele, 2007).

Consistent with activity of the melanin biosynthesis pathway downstream of tyrosinase (TYR) being the key determinant in the Raman spectra observed in cells of the melanocyte lineage we observed a subdued UV response in keratinocytes (COCA) very similar to the one observed in undifferentiated melanoblasts (melb-a) with a delayed (24 hours) statistically significant reduction in phenylalanine post UVA exposure Figure 5a and an immediate (from one hour) and sustained (up to 24-hours) reduction in phenylalanine and tyrosine post UVB exposure Figure 4b. Exposure to the UVA-UVB mixed light source resulted in an immediate (one hour) and transient (up to three hours) reduction in tyrosine Figure 4c. We observed inconsistent changes in the DOPA and melanin peaks in keratinocytes (COCA) likely attributable to noise caused by the very low basal level of DOPA in the control samples Figure 4a.

Differentiated melanocytes but not melanoblasts, melanoma cells or keratinocytes demonstrate a photoprotective responses to UVR

The photoprotective effects of β-carotene have been attributed to its free radical/reactive oxygen species (ROS) scavenging abilities as well as direct absorption of UV at 400 nm (Moshell and Bjornson, 1977; Alaluf *et al.*, 2002). Melanocytes have been shown to preferentially absorb β-carotene in culture (Andersson, Vahlquist and Rosdahl, 2001). Consistent with this, we observed a distinct β-carotene Raman peak in melanocytes (melan-a) that was absent from the spectra of melanoblasts (melb-a) melanoma (B16F10) cells and keratinocytes (COCA) (Figure 1b, Supplementary Table 1). In response to UVR we observed a statistically significant increase in the β-carotene peak in melanocytes (between one and 24

hours post UV) in response to UVA, UVB and mixed UVA/UVB light sources (Figure 6b). We therefore hypothesised that β-carotene may be performing a cell-type specific photoprotective function in melanocytes protecting proteins and lipids from oxidative damage. To evaluate this hypothesis we investigated changes in the Raman peaks for lipids (1300cm^{-1} peak) and amide I (protein peaks at 1650cm^{-1}) in our Raman spectra as biomarkers of oxidative damage (Figure 6a-d).

We observed a rapid (one to three hours) and statistically significant reduction in the amide I peak in melanoblasts (melb-a) in response to UVA and UVB (Figure 6a) which appeared absent or dampened in melanocytes (melan-a) (Figure 6b). Furthermore, we observed a rapid (within one hour) statistically significant reduction in the lipid peak in response to UVA and a rapid (within one hour) statistically significant increase in the lipid peak in response to a mixed UVA/UVB light source in melanoblasts (Figure 6a). No changes in the lipid peak were observed in melanocytes (Figure 6b). These results suggest differentiated melanocytes are better protected against the effects of UVR than melanoblasts. Consistent with a more heterogeneous population of cells in melanoma, no clear trends in the lipid or amide I peaks were observed in melanoma (B16F10) cells (Figure 6c). Lipid levels have previously been shown to increase in human keratinocytes post UVA and UVB dual irradiation (Olivier *et al.*, 2017). Consistent with this, here we observed rapid (from 1-3 hours) and sustained (at least 24 hours) statistically significant increases in the lipid peak in response to UVA, UVB and our mixed UVA/UVB light source in keratinocytes (COCA) (Figure 6d).

Melanoblasts, melanoma cells and keratinocytes but not melanocytes demonstrate changes in keratin levels on UV exposure

Raman peaks consistent with keratin were present in keratinocytes (COCA) and melanoblasts (melb-a). We observed a rapid (within 1 hour) and sustained (up to 24 hours) statistically significant increase in the Raman peak for keratin in keratinocytes (COCA) after UVA treatment with similar rapid (one to three hours) and transient (less than six hours) statistically significant increases after UVB and combined UVA/UVB treatments in these cells (Figure 6d). Melanoblasts displayed a significant reduction in keratin after individual UVA and UVB treatments but an immediate (from one hour) and sustained (up to 24 hours) statistically significant increase in keratin after exposure to the dual UVA/UVB light source (Figure 6a). Melanoma cells (B16F10) but not melanocytes (melan-a) also exhibited a keratin peak and demonstrated a delayed (6-24 hours) statistically significant increase after UVB treatment (Figure 6c).

DISCUSSION

Raman spectroscopy is a valuable technique in skin cell research with the potential to discriminate biochemically between cell types in a label free manner (Brauchle *et al.*, 2014; Moncada *et al.*, 2016). Further to previous studies (Silveira *et al.*, 2012; Brauchle *et al.*, 2014), we show here that live single cell Raman fingerprinting can delineate the differentiation status of cells of the melanocyte lineage and discriminate these cells from keratinocytes. We demonstrate the utility of Raman spectroscopy performed on cells grown in a controlled environmental chamber, as a unique tool to probe the melanin biosynthesis pathway and its immediate response to UVR and reveal rapid and opposing responses to UVA and UVB irradiation by melanocytes.

Raman fingerprinting demonstrates that melanoma cells are phenotypically

Previous reports have discriminated between malignant melanoma cells and their wildtype counterparts using Raman spectroscopy (Silveira Jr. et al., 2012; Brauchle et al., 2014). Our Raman spectra appear consistent with those previously reported for melanocytes and melanomas cells (Gniadecka *et al.*, 2004; Silveira *et al.*, 2012; Feng *et al.*, 2017), while our spectra for melanoblasts and keratinocytes are consistent with their inability to synthesise melanin (Sviderskaya, Wakeling and Bennett, 1995). Our PCA analysis of the Raman spectra of melanoblasts, melanocytes, melanoma cells and keratinocytes showed that melanoblasts, melanocytes and keratinocytes represent biochemically homogeneous populations. However melanoma cells are a biochemically heterogeneous population positioned between undifferentiated melanoblasts and differentiated melanocytes, consistent with their known phenotypic heterogeneity and the reactivation of their embryonic transcriptome (Vandamme and Berx, 2014; Marie *et al.*, 2020). Further study is therefore warranted to address whether this method can be used to predict the position of a melanoma cell on the recently described two-dimensional differentiation trajectory of melanoma subtypes (Tsoi *et al.*, 2018) which may allow exploitation of these properties to increase immune therapy efficacy.

Rapid and opposing effects of UVA and UVB irradiation on the melanin biosynthesis pathway in melanocytes

We show here the utility of Raman spectroscopy as a tool to detect and sensitively measure changes in components of the melanin biosynthesis pathway in response to UVR over a smaller time-frame than is possible with conventional methods.. Therefore, melanocytes appear to mount a sustained and rapid response to UV irradiation in the melanin biosynthesis pathway with decreases in phenylalanine and increases in tyrosine, DOPA and melanin post UVB and an increase in phenylalanine and decrease in tyrosine, DOPA and melanin post UVA (Figure 1).

UVA exposure has long been understood to result in immediate pigment darkening within a few hours of exposure by acting on pre-existing melanin and by *de novo* melanin synthesis stimulated by calcium mobilisation in human epidermal melanocytes (Miyamura *et al.*, 2011; Wicks *et al.*, 2011). The reduction in melanin post UVA and accumulation of phenylalanine observed here may be consistent with a rapid tanning response resulting in the export of melanosomes from the cytosol and a subsequent block in synthesis because of their loss leading to accumulation of phenylalanine. This is consistent with reports UVA induces a redistribution of melanosomes in the skin (Lavker and Kaidbey, 1982). We do not see the rapid accumulation of melanin overserved in human epidermal melanocytes (Wicks *et al.*, 2011) . UVB has long been demonstrated to cause a delayed tanning response mediated through DNA damage induced *de novo* tyrosinase production (Eller, Ostrom and Gilchrest, 1996; Cui *et al.*, 2007). We were surprised here then to see such a rapid and profound UVB mediated response with rapid and sustained increases in Tyrosine, DOPA and Melanin (confirmed by intracellular measurements) and reductions in phenylalanine suggesting a previously overlooked mechanism independent of DNA damage is acting immediately after UVB exposure in mouse melanocytes.

Melanocytes uniquely harbour β-carotene with a possible role in photoprotection

β-carotene's singlet oxygen scavenging abilities underly its role in photoprotection against UV-induced lipid peroxidation, DNA damage and protein oxidation (Alaluf et al., 2002; Stephen, Coetzee and Perrett, 2011). Consistent with previous reports, (Andersson, Vahlquist and Rosdahl, 2001) we observe a melanocyte specific accumulation β-carotene. Levels increased significantly in response to UVA, UVB and a mixed UVA/UVB light source. Consistent with its proposed mechanism of photoprotection the presence of β-carotene also appeared to

correlate with an apparent stabilisation in the peaks of amide I and lipid in melanocytes, whereas these biomarkers appeared to change dramatically in response to UVR in the other cell types studied.

CONCLUSION

By comparing Raman spectra between melanoblasts, melanocytes, melanoma cells and keratinocytes and their response to UVR we have defined a reference biochemical response signature for each that can be attributed to their biological function and shown that we can use this to determine differentiation status. In doing so we have demonstrated the utility of Raman spectroscopy as a tool to probe the melanin biosynthesis pathway and uncovered hitherto undescribed immediate responses to UVA and UVB irradiation in melanocytes. The ability to measure biochemical changes in a sensitive time-dependent study will be very beneficial to continued research in the study of melanoma.

MATERIALS AND METHODS:

Cell culture

Mouse melan-a cells were cultured in RPMI 1640 (21875-034, Invitrogen) supplemented with 10% (v/v) FCS and 200nM TPA. melb-a cells were cultured in RPMI 1640 (21875-034, Invitrogen) supplemented with 10% (v/v) FCS, 40pM FGF2 and 20ng/ml mSCF. B16F10 cells were cultured in RPMI 1640 (21875-034, Invitrogen) supplemented with 5% (v/v) FCS. COCA cells were cultured in CnT-07 (CELLnTEC). Cells were incubated at 37°C in humidified air containing 5% (v/v) CO_2.

Raman spectroscopy

Cells were seeded on CaF_2 disks in 24 well plates for 24 hours before the media was changed to phenol-free media for 24 hours prior to UV radiation. Cells were irradiated with 100KJ/m2 UVA, 1000J/m^2 UVA and UVB or 100J/m2 UVB before spectra acquired at 1, 3, 6, 16 and 24 hours post radiation as well as from an untreated control. Raman spectra were acquired using an InVia Raman microspectrometer (Renishaw plc, Gloucestershire, UK) using a 785nm laser at a spectral range of 600-1700cm^{-1}. Samples were set up in a prewarmed incubator (Okolab, Ottaviano, NA, Italy) to 37°C 5% (v/v) CO_2 and spectra acquired using a 60x water immersion objective. Samples were kept at 37°C for the duration of the experiment. Spectra was collected at 2 seconds with 9 accumulations (18 seconds total) at 100% laser power. There was a total of 18 spectra collected across 3 independent runs with spectra from 6 individual cells collected each run. Cells were selected randomly by moving diagonally along and collecting spectra every 10th cell to ensure spread across the disc and that no overlap occured. Data collected was baseline corrected using a polynomial method order 3 and smoothed using P=0.001, λ=105 before vector normalising. Principal component analysis was performed in MatlabR2018A

(The Mathworks, NA, USA) using (which code was it Lorna's or mine? Add refs as appropriate).

Cell Viability

Viability was measured using Cell Titer Glo (promega) following spectra acquisition. CaF_2 disks were transferred to a 24 well plate, along with control disks that had not been used for spectral acquisition, and diluted Cell Titer Glo was added to cells for 10 minutes before scraping and transferring to a white 96 well plate and bioluminescence measured as relative light units using a Perkin Elmer Wallac 1420 Victor2 microplate reader.

Measurement of the amount of intracellular melanin

Cells were UV-irradiated as described above. Subsequently they were washed in PBS and trypsinised before counting, then pelleted at 1000 RPM for 3 minutes. 100µL of melanin lysis buffer (90% 1M NaOH and 10% DMSO) was added to each pellet before incubation at 80°C for 90 minutes. Lysed pellets where transferred to a 96 well plate and their absorbance read at 490nm on a Perkin Elmer Wallac 1420 Victor2 microplate reader. A standard curve was obtained by diluting synthetic melanin (Sigma, Poole, UK) 0 to 1µg/mL to enable to concentration of melanin to be determined per cell.

Statistical significance

All statistical tests were performed in SPSS or using the 'R' statistics package, an open source software package based on the 'S' programming language (http://www.R-project.org). To analyse the Raman data presented in Figures 2-6 data was normalised individually for each peak across all cell types and conditions. A one-way analysis of variance (ANOVA) was performed across the six time points for each combination of cell type and UVA treatment

followed by pairwise comparisons by Tukey's Honestly Significant Difference test (TukeyHSD). Therefore a significant ANOVA *P* value is required in order to consider any significant TukeyHSD *P* value indicated in the matrices. For the qPCR data in Figures 2 and 3, data was analysed using SPSS. A one-way analysis of variance (ANOVA) was performed across the 3 time points for each cell type and UVR treatment this was followed by pairwise Dunnett's post hoc tests. Significant differences between control and time were evaluated with *p values ≤0.05 as indicated on the graphs. Error bars denote ± s.d. (standard deviation) N=3.

RT-qPCR Analysis

Quantitative reverse transcriptase polymerase chain reaction (RT-qPCR) was performed by first extracting total RNA from melan-A and B16F10 cells using the RNAeasy kit (Qiagen, Crawley, UK). following the manufacturer's instructions. Reverse transcription of 1 µg RNA, oligo dT18, M-MLV reverse transcriptase, RNase OUT (Invitrogen, Thermo Fisher Scientific) was performed to synthesise cDNA. For RT-qPCR 10ng cDNA was used along with 12.5 µl of 2X Power SYBR® Green master mix (Applied Biosystems, Warrington, UK) and 400nM primers (Sigma, Poole, UK). Primer sequences listed in supplementary table 2. Reactions were performed on a BioRad CFX RT-qPCR machine using parameters: 50°C for 2 min and 95°C for 10 min followed by 40cycles of 95°C for 15 s and 60°C for 1 min. Cycle threshold (CT) values were generated for each mRNA sample and compared to their respective actin control to determine gene expression changes using the comparative CT (2−ΔΔCT) method (Livak and Schmittgen, 2001).

DATA AVAILABILITY STATEMENT

The data that support the findings of this study will be available after publication at https://www.research.lancs.ac.uk/portal/en/people/richard-mort(ed9f7471-68c9-4816-97a9-58f8f44c1f1d).html and from the corresponding author on reasonable request.

ORCIDs

Emma L. Wilkinson 0000-0002-7261-3338

Lorna Ashton 0000-0002-1323-6309

Jemma G. Kerns 0000-0001-5213-8392

Sarah L. Allinson 0000-0003-1937-5550

Richard L. Mort 0000-0002-3566-8217

CONFLICT OF INTEREST STATEMENT

The authors state no conflict of interest.

ACKNOWLEDGMENTS

This work was supported by a project grant from North West Cancer Research (Grant CR1132).

AUTHOR CONTRIBUTIONS STATEMENT

Conceptualization: RLM, SLA, JGK, LA; Data Curation: RLM, EW, JGK; Formal Analysis: ELW, RLM; Funding Acquisition: RLM, SLA; Investigation: ELW; Methodology: RLM, JGK; Project Administration: ELW; Resources: RLM, SLA, JGK, LA; Software: JGK, RLM, ELW; Supervision: RLM; Validation: ELW; Visualization: ELW, RLM; Writing - Original Draft Preparation: ELW, RLM; Writing - Review and Editing: RLM, ELW, SLA, LA, JGK.

REFERENCES :

Alaluf, S. *et al.* (2002) 'Dietary Carotenoids Contribute to Normal Human Skin Color and UV Photosensitivity', *The Journal of Nutrition*. Oxford Academic, 132(3), pp. 399–403. doi: 10.1093/jn/132.3.399.

Andersson, E., Vahlquist, A. and Rosdahl, I. (2001) 'Beta-carotene uptake and bioconversion to retinol differ between human melanocytes and keratinocytes.', *Nutrition and cancer*. Nutr Cancer, 39(2), pp. 300–6. doi: 10.1207/S15327914nc392_21.

BACHEM, A. (1955) ‘Time factors of erythema and pigmentation, produced by ultraviolet rays of different wavelengths.’, *The Journal of investigative dermatology*. J Invest Dermatol, 25(4), pp. 215–8. doi: 10.1038/jid.1955.123.

Baldea, I., Mocan, T. and Cosgarea, R. (2009) ‘The role of ultraviolet radiation and tyrosine stimulated melanogenesis in the induction of oxidative stress alterations in fair skin melanocytes.’, *Experimental oncology*, 31(4), pp. 200–8. Available at: http://www.ncbi.nlm.nih.gov/pubmed/20010534 (Accessed: 1 August 2019).

Bose, B., Agarwal, S. and Chatterjee, S. N. (1989) ‘UV-A induced lipid peroxidation in liposomal membrane.’, *Radiation and environmental biophysics*, 28(1), pp. 59–65. Available at: http://www.ncbi.nlm.nih.gov/pubmed/2919226 (Accessed: 1 August 2019).

Bose, B., Agarwal, S. and Chatterjee, S. N. (1990) ‘Membrane lipid peroxidation by UV-A: mechanism and implications.’, *Biotechnology and applied biochemistry*, 12(5), pp. 557–61. Available at: http://www.ncbi.nlm.nih.gov/pubmed/2288712 (Accessed: 1 August 2019).

Brauchle, E. *et al.* (2014) ‘Raman spectroscopy as an analytical tool for melanoma research’, *Clinical and Experimental Dermatology*, 39(5), pp. 636–645. doi: 10.1111/ced.12357.

Cichorek, M. *et al.* (2013) ‘Skin melanocytes: Biology and development’, *Postepy Dermatologii i Alergologii*, 30(1), pp. 30–41. doi: 10.5114/pdia.2013.33376.

Cui, R. *et al.* (2007) ‘Central Role of p53 in the Suntan Response and Pathologic Hyperpigmentation’, *Cell*, 128(5), pp. 853–864. doi: 10.1016/j.cell.2006.12.045.

Diwakar, G. *et al.* (2008) ‘Neurofibromin as a regulator of melanocyte development and differentiation’, *Journal of Cell Science*, 121(2), pp. 167–177. doi: 10.1242/jcs.013912.

Eller, M. S., Ostrom, K. and Gilchrest, B. A. (1996) ‘DNA damage enhances melanogenesis’, *Proceedings of the National Academy of Sciences of the United States of America*. National Academy of Sciences, 93(3), pp. 1087–1092. doi: 10.1073/pnas.93.3.1087.

Erdei, E. and Torres, S. M. (2010) ‘A new understanding in the epidemiology of melanoma.’, *Expert review of anticancer therapy*. NIH Public Access, 10(11), pp. 1811–23. doi: 10.1586/era.10.170.

Feng, X. *et al.* (2017) ‘Raman active components of skin cancer’, *Biomed Opt Express*. 2017/07/01, 8(6), pp. 2835–2850. doi: 10.1364/BOE.8.002835.

FIDLER, I. J. (1973) ‘Selection of Successive Tumour Lines for Metastasis’, *Nature New Biology*. Nature Publishing Group, 242(118), pp. 148–149. doi: 10.1038/newbio242148a0.

Filipe, P. *et al.* (2013) ‘Plasma lipoproteins as mediators of the oxidative stress induced by UV light in human skin: a review of biochemical and biophysical studies on mechanisms of apolipoprotein alteration, lipid peroxidation, and associated skin cell responses’, *Oxid Med Cell Longev*. 2013/06/06, 2013, p. 285825. doi: 10.1155/2013/285825.

FITZPATRICK, T. B. and BREATHNACH, A. S. (1963) ‘DAS EPIDERMALE MELANIN-EINHEIT-SYSTEM.’, *Dermatologische Wochenschrift*, 147, pp. 481–489. Available at: http://www.ncbi.nlm.nih.gov/pubmed/14172128 (Accessed: 1 August 2019).

Gillbro, J. M. *et al.* (2004) ‘Autocrine catecholamine biosynthesis and the beta-adrenoceptor signal promote pigmentation in human epidermal melanocytes.’, *The Journal of investigative dermatology*. J Invest Dermatol, 123(2), pp. 346–53. doi: 10.1111/j.0022-202X.2004.23210.x.

Gniadecka, M. *et al.* (2004) 'Melanoma diagnosis by Raman spectroscopy and neural networks: structure alterations in proteins and lipids in intact cancer tissue.', *The Journal of investigative dermatology*, 122(2), pp. 443–9. doi: 10.1046/j.0022-202X.2004.22208.x.

Grimm, S., Höhn, A. and Grune, T. (2012) 'Oxidative protein damage and the proteasome.', *Amino acids*. Amino Acids, 42(1), pp. 23–38. doi: 10.1007/s00726-010-0646-8.

Hönigsmann, H. *et al.* (1986) 'Immediate pigment darkening phenomenon. A reevaluation of its mechanisms.', *The Journal of investigative dermatology*. J Invest Dermatol, 87(5), pp. 648–52. doi: 10.1111/1523-1747.ep12456326.

Ikehata, H. and Ono, T. (2011) 'The mechanisms of UV mutagenesis.', *Journal of radiation research*. J Radiat Res, 52(2), pp. 115–25. doi: 10.1269/jrr.10175.

Jimbow, K. *et al.* (1976) 'Some Aspects Of Melanin Biology: 1950–1975', *Journal of Investigative Dermatology*. Elsevier, 67(1), pp. 72–89. doi: 10.1111/1523-1747.EP12512500.

Kerwin, B. A. and Remmele, R. L. (2007) 'Protect from light: photodegradation and protein biologics.', *Journal of pharmaceutical sciences*. J Pharm Sci, 96(6), pp. 1468–79. doi: 10.1002/jps.20815.

Kobayashi, N. *et al.* (1998) 'Supranuclear Melanin Caps Reduce Ultraviolet Induced DNA Photoproducts in Human Epidermis', *Journal of Investigative Dermatology*. Elsevier, 110(5), pp. 806–810. doi: 10.1046/J.1523-1747.1998.00178.X.

Kollias, N., Ruvolo Jr, E. and Sayre, R. M. (2011) 'The Value of the Ratio of UVA to UVB in Sunlight', *Photochemistry and Photobiology*, 87(6), pp. 1474–1475. doi: 10.1111/j.1751-1097.2011.00980.x.

Lavker, R. M. and Kaidbey, K. H. (1982) 'Redistribution of melanosomal complexes within keratinocytes following UV-A irradiation: a possible mechanism for cutaneous darkening in man', *Archives of dermatological research*. Arch Dermatol Res, 272(3–4), pp. 215–228. doi: 10.1007/BF00509049.

Linos, E. *et al.* (2009) 'Increasing burden of melanoma in the United States.', *The Journal of investigative dermatology*. J Invest Dermatol, 129(7), pp. 1666–74. doi: 10.1038/jid.2008.423.

Livak, K. J. and Schmittgen, T. D. (2001) 'Analysis of Relative Gene Expression Data Using Real-Time Quantitative PCR and the 2−ΔΔCT Method', *Methods*. Academic Press, 25(4), pp. 402–408. doi: 10.1006/METH.2001.1262.

Maddodi, N., Jayanthy, A. and Setaluri, V. (2012) 'Shining light on skin pigmentation: the darker and the brighter side of effects of UV radiation', *Photochem Photobiol*. 2012/03/13, 88(5), pp. 1075–1082. doi: 10.1111/j.1751-1097.2012.01138.x.

Marie, K. L. *et al.* (2020) 'Melanoblast transcriptome analysis reveals pathways promoting melanoma metastasis', *Nature Communications*, 11(1). doi: 10.1038/s41467-019-14085-2.

Miyamura, Y. *et al.* (2011) 'The deceptive nature of UVA tanning versus the modest protective effects of UVB tanning on human skin.', *Pigment cell & melanoma research*. Pigment Cell Melanoma Res, 24(1), pp. 136–47. doi: 10.1111/j.1755-148X.2010.00764.x.

Moncada, B. *et al.* (2016) 'Raman spectroscopy analysis of the skin of patients with melasma before standard treatment with topical corticosteroids, retinoic acid, and hydroquinone mixture', *Skin Research and Technology*, 22(2), pp. 170–173. doi: 10.1111/srt.12245.

Mort, R. L., Jackson, I. J. and Elizabeth Patton, E. (2015) 'The melanocyte lineage in development and disease', *Development (Cambridge)*, 142(4). doi: 10.1242/dev.106567.

Moshell, A. N. and Bjornson, L. (1977) 'Photoprotection in erythropoietic protoporphyria: mechanism of photoprotection by beta carotene.', *The Journal of investigative dermatology*. J Invest Dermatol, 68(3), pp. 157–60. doi: 10.1111/1523-1747.ep12492479.

Nordlund, J. J., Ackles, A. E. and Traynor, F. F. (1981) 'The Proliferative and Toxic Effects of Ultraviolet Light and Inflammation of Epidermal Pigment Cells', *Journal of Investigative Dermatology*, 77(4), pp. 361–368. doi: 10.1111/1523-1747.ep12493267.

Olivier, E. *et al.* (2017) 'Lipid deregulation in UV irradiated skin cells: Role of 25-hydroxycholesterol in keratinocyte differentiation during photoaging', *Journal of Steroid Biochemistry and Molecular Biology*. doi: 10.1016/j.jsbmb.2016.05.015.

Rosdahl, I. K. (1979) 'Local and Systemic Effects on the Epidermal Melanocyte Population in UV-irradiated Mouse Skin', *Journal of Investigative Dermatology*, 73(4), pp. 306–309. doi: 10.1111/1523-1747.ep12531840.

Sato, T. and Kawada, A. (1972) 'Mitotic Activity of Hairless Mouse Epidermal Melanocytes: Its Role in the Increase of Melanocytes During Ultraviolet Radiation', *Journal of Investigative Dermatology*, 58(6), pp. 392–395. doi: 10.1111/1523-1747.ep12540628.

Schallreuter, K. *et al.* (1994) 'Regulation of melanin biosynthesis in the human epidermis by tetrahydrobiopterin', *Science*, 263(5152), pp. 1444–1446. doi: 10.1126/science.8128228.

Schallreuter, K. U. *et al.* (1992) 'Production of catecholamines in the human epidermis.', *Biochemical and biophysical research communications*. Biochem Biophys Res Commun, 189(1), pp. 72–8. doi: 10.1016/0006-291x(92)91527-w.

Schallreuter, K. U. *et al.* (1995) 'Catecholamines in human keratinocyte differentiation.', *The Journal of investigative dermatology*. J Invest Dermatol, 104(6), pp. 953–7. doi: 10.1111/1523-1747.ep12606218.

Segrelles, C. *et al.* (2011) 'Establishment of a murine epidermal cell line suitable for in vitro and in vivo skin modelling', *BMC Dermatology*. BioMed Central, 11, p. 9. doi: 10.1186/1471-5945-11-9.

Silveira, L. *et al.* (2012) 'Discriminating model for diagnosis of basal cell carcinoma and melanoma in vitro based on the Raman spectra of selected biochemicals.', *Journal of biomedical optics*, 17(7), p. 077003. doi: 10.1117/1.JBO.17.7.077003.

Sviderskaya, E. V., Wakeling, W. F. and Bennett, D. C. (1995) 'A cloned, immortal line of murine melanoblasts inducible to differentiate to melanocytes', *Development*, 121(5), pp. 1547–1557.

Tsoi, J. *et al.* (2018) 'Multi-stage Differentiation Defines Melanoma Subtypes with Differential Vulnerability to Drug-Induced Iron-Dependent Oxidative Stress.', *Cancer cell*. NIH Public Access, 33(5), pp. 890-904.e5. doi: 10.1016/j.ccell.2018.03.017.

Vandamme, N. and Berx, G. (2014) 'Melanoma cells revive an embryonic transcriptional network to dictate phenotypic heterogeneity.', *Frontiers in oncology*. Front Oncol, 4, p. 352. doi: 10.3389/fonc.2014.00352.

Wallingford, S. C. *et al.* (2013) 'Regional melanoma incidence in England, 1996-2006: reversal of north-south latitude trends among the young female population', *British Journal*

of Dermatology, 169(4), pp. 880–888. doi: 10.1111/bjd.12460.

Wicks, N. L. *et al.* (2011) 'UVA phototransduction drives early melanin synthesis in human melanocytes', *Current Biology*. Cell Press, 21(22), pp. 1906–1911. doi: 10.1016/j.cub.2011.09.047.

FIGURE LEGENDS:

Figure 1 Live Raman spectroscopy can discriminate between cell types and differentiation status. Raman spectra (n = 9 for each cell type) were acquired from melanocytes (melan-a), melanoblasts (MelbA), melanoma cells (B16F10) and keratinocytes (COCA). Cells were grown on CaF_2 disks in phenol red free medium prior to acquisition at 785nm. A principal component analysis (PCA) was then conducted. (a) Bright field images of the cell types used. (b) The mean Raman spectra (offset for clarity) for each cell type differed qualitatively. (c) A scatter plot of the principal component vectors PC1 (98.27%) and PC2 (1.05%) showing tight grouping of melanoblasts, melanocytes and keratinocytes with a more heterogeneous melanoma population. (d) Plot of the PC1 and PC2 vectors - the ten principal Raman peaks are labelled with arrows on (b). Scale bar in A = 200 µm. Numbers in (b): 1 = Lipid, 2 = Phenylalanine, 3 = Phospholipids/Tryptophan, 4 = Lipid, 5 = DOPA, 6 = β-carotene, 7 = Keratin, 8 = Melanin, 9 = Tyrosine, 10 = Amide I.

Figure 2 Distinct UVA and UVB responses in the melanin synthesis pathway in melan-a melanocytes. Cells were grown on CaF_2 disks and irradiated with 100KJ/m^2 UVA, 100J/m^2 UVB or 1000J/m^2 UVA + UVB. Raman spectra (at 785nm) were acquired at 1, 3, 6, 16 and 24 hours post irradiation. (a-c) Time course of log_2 fold (F) change (Log2-FC) and pairwise Tukey's honestly significant difference (TukeyHSD) comparing response (to UVA, UVB or UVA/UVB) to 0 hours control for phenylalanine, tyrosine, l-DOPA and melanin (n = 18 spectra for each square). Significance level for a one-way analysis of variance (ANOVA) is indicated at the end of each series (*<0.05, **<0.01, ***<0.001, ****<0.0001). (d-e) qRT-PCR time course analysis of fold change in *Tyr, Dct, Tyrp1* and *Mitf* expression (mean ± s.d, n=3) after. (f) Time course of intracellular melanin content (mean ± 95% CI, n = 3) after treatment.

Figure 3 Similar UVA and UVB responses in the melanin synthesis pathway in B16F10 melanoma cells. Cells were grown on CaF2 disks and irradiated with 100KJ/m2 UVA, 100J/m2 UVB or 1000J/m2 UVA + UVB. Raman spectra (at 785nm) were acquired at 1, 3, 6, 16 and 24 hours post irradiation. (a-c) Time course of $\log_2$ fold (F) change (Log2-FC) and pairwise Tukey's honestly significant difference (TukeyHSD) comparing response (to UVA, UVB or UVA/UVB) to 0 hours control for phenylalanine, tyrosine, l-DOPA and melanin (n = 18 spectra for each square). Significance level for a one-way analysis of variance (ANOVA) is indicated at the end of each series (*<0.05, **<0.01, ***<0.001, ****<0.0001). (d-e) qRT-PCR time course analysis of fold change in Tyr, Dct, Tyrp1 and Mitf expression (mean ± s.d, n=3) after. (f) Time course of intracellular melanin content (mean ± 95% CI, n = 3) after treatment.

Figure 4 UVA and UVB responses in the melanin synthesis pathway in melanoblasts (melb-a). Cells were grown on CaF2 disks and irradiated with 100KJ/m2 UVA, 100J/m2 UVB or 1000J/m2 UVA + UVB. Raman spectra (at 785nm) were acquired at 1, 3, 6, 16 and 24 hours post irradiation. (a-c) Time course of $\log_2$ fold (F) change (Log2-FC) and pairwise Tukey's honestly significant difference (TukeyHSD) comparing response (to UVA, UVB or UVA/UVB) to 0 hours control for phenylalanine, tyrosine, l-DOPA and melanin (n = 18 spectra for each square). Significance level for a one-way analysis of variance (ANOVA) is indicated at the end of each series (*<0.05, **<0.01, ***<0.001, ****<0.0001).

Figure 5 UVA and UVB responses in the melanin synthesis pathway in keratinocytes (COCA). Cells were grown on CaF2 disks and irradiated with 100KJ/m2 UVA, 100J/m2 UVB or 1000J/m2 UVA + UVB. Raman spectra (at 785nm) were acquired at 1, 3, 6, 16 and 24 hours post irradiation(a-c) Time course of $\log_2$ fold (F) change (Log2-FC) and pairwise Tukey's

honestly significant difference (TukeyHSD) comparing response (to UVA, UVB or UVA/UVB) to 0 hours control for phenylalanine, tyrosine, l-DOPA and melanin (n = 18 spectra for each square). Significance level for a one-way analysis of variance (ANOVA) is indicated at the end of each series (*<0.05, **<0.01, ***<0.001, ****<0.0001).

Figure 6. Heterogeneous responses of melanoblasts, melanocytes, melanoma cells and keratinocytes to UVR. Cells were grown on CaF2 disks and irradiated with 100KJ/m2 UVA, 100J/m2 UVB or 1000J/m2 UVA + UVB. Raman spectra (at 785nm) were acquired at 1, 3, 6, 16 and 24 hours post irradiation. (a-d) Time course of log2 fold (F) change (Log2-FC) and pairwise Tukey's honestly significant difference (TukeyHSD) test comparing response to 0 hours control for amide I, lipid, keratin, and β-carotene (n = 18 spectra for each square). Significance level for a one-way analysis of variance (ANOVA) is indicated at the end of each series (*<0.05, **<0.01, ***<0.001, ****<0.0001).

GRAPHICAL ABSTRACT:

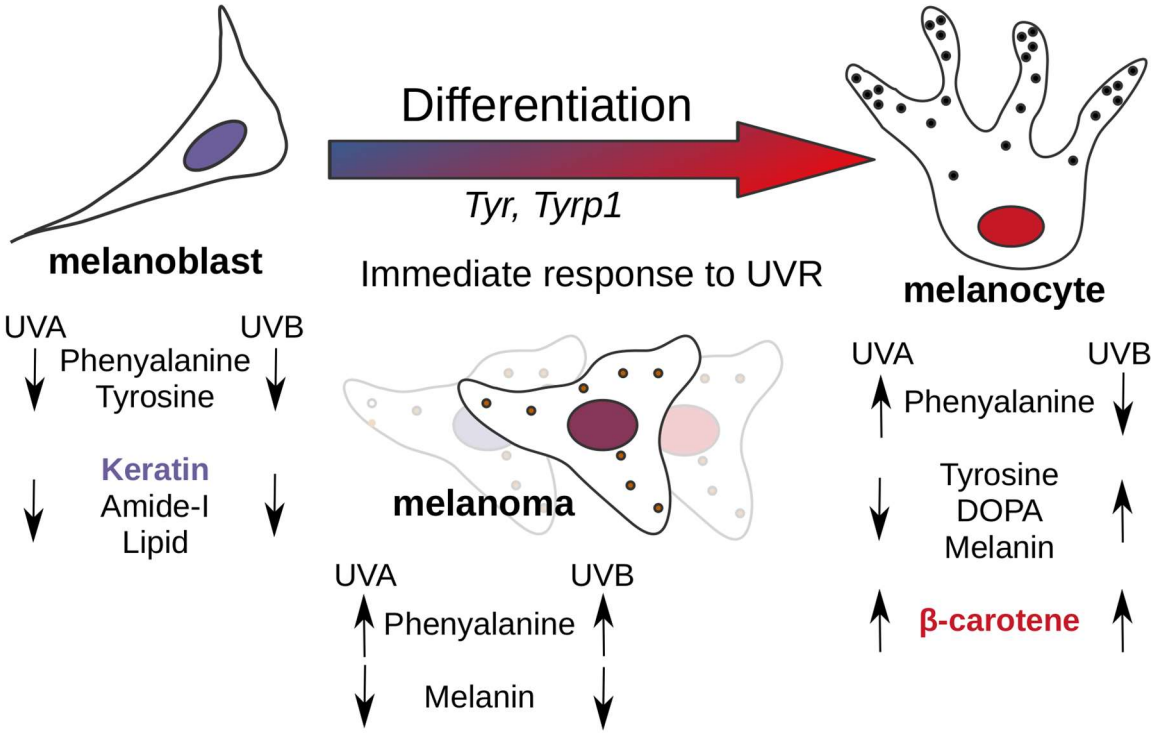

FIGURE 1:

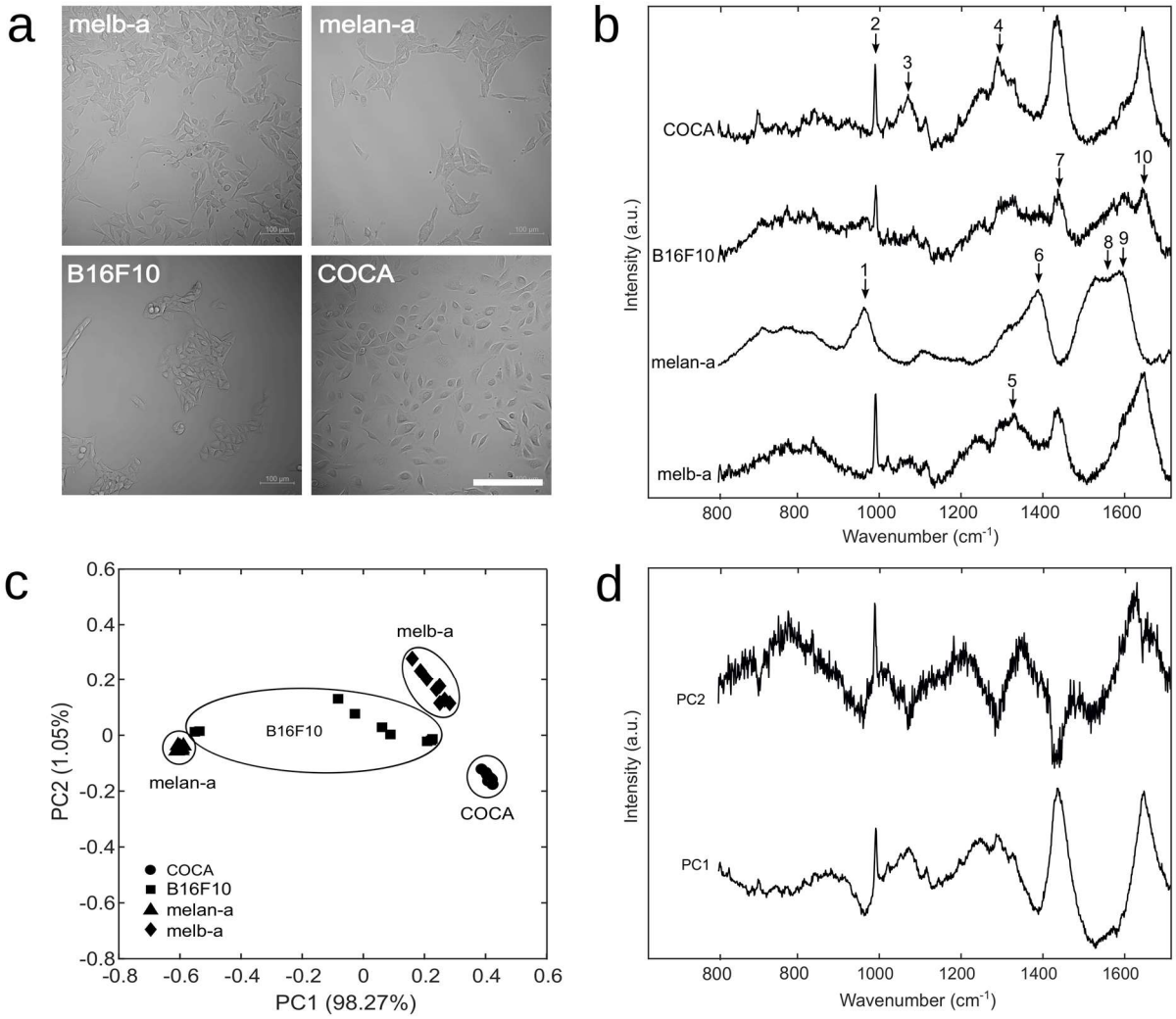
a
melb-a
melan-a
B16F10
COCA
b
COCA
B16F10
melan-a
melb-a
Intensity (a.u.)
Wavenumber (cm-1)
c
melb-a
B16F10
melan-a
COCA
COCA
B16F10
melan-a
melb-a
PC2 (1.05%)
PC1 (98.27%)
d
PC2
PC1
Intensity (a.u.)
Wavenumber (cm-1)

FIGURE 2:

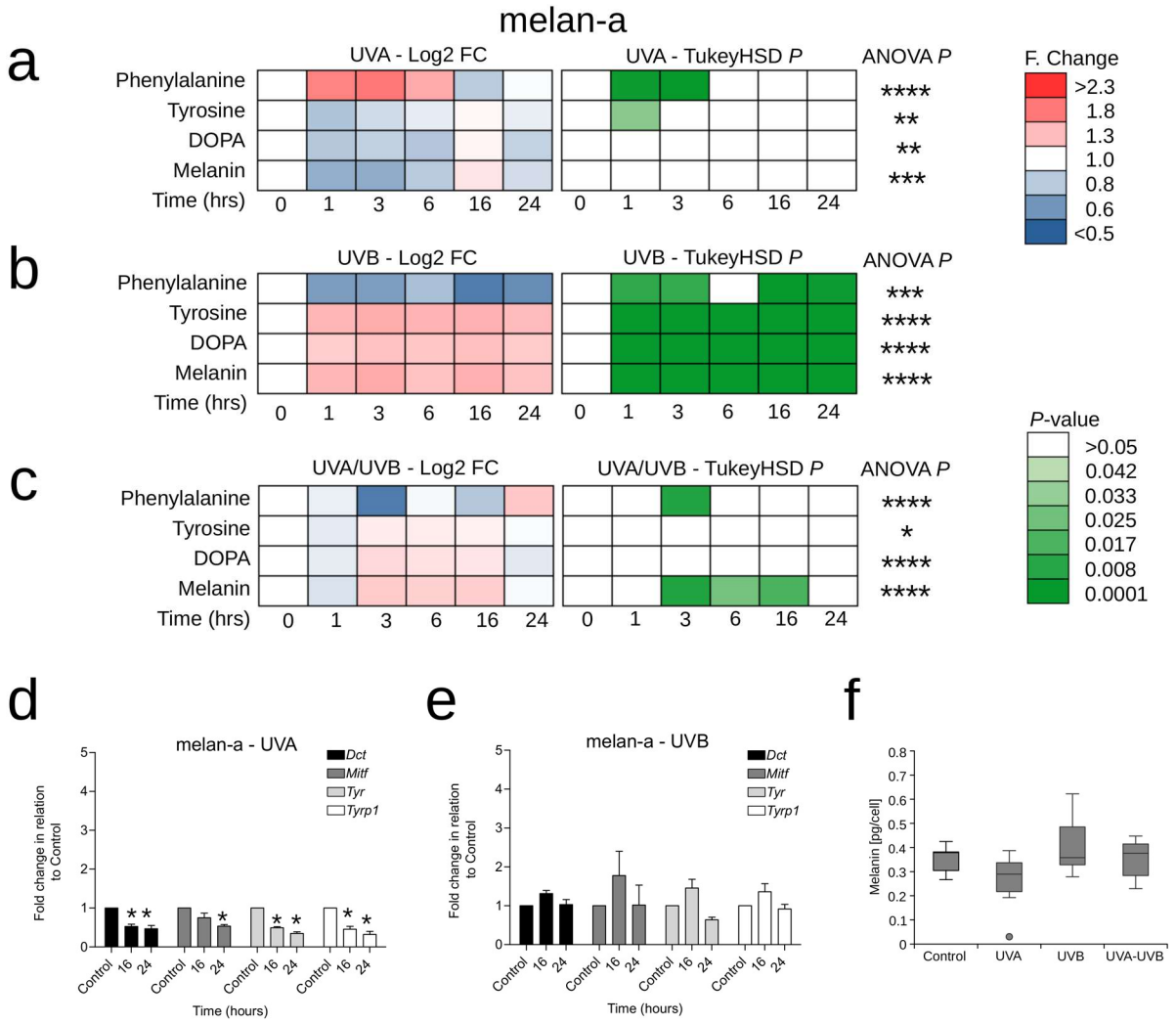
melan-a
a
UVA - Log2 FC
UVA - TukeyHSD P
ANOVA P
Phenylalanine
Tyrosine
DOPA
Melanin
Time (hrs)
0 1 3 6 16 24
****
**
**
***
F. Change
>2.3
1.8
1.3
1.0
0.8
0.6
<0.5
b
UVB - Log2 FC
UVB - TukeyHSD P
***
****
****
****
P-value
>0.05
0.042
0.033
0.025
0.017
0.008
0.0001
c
UVA/UVB - Log2 FC
UVA/UVB - TukeyHSD P
****
*
****
****
d
melan-a - UVA
Dct
Mitf
Tyr
Tyrp1
Fold change in relation to Control
Control 16 24
Time (hours)
e
melan-a - UVB
f
Melanin [pg/cell]
Control
UVA
UVB
UVA-UVB

FIGURE 3:

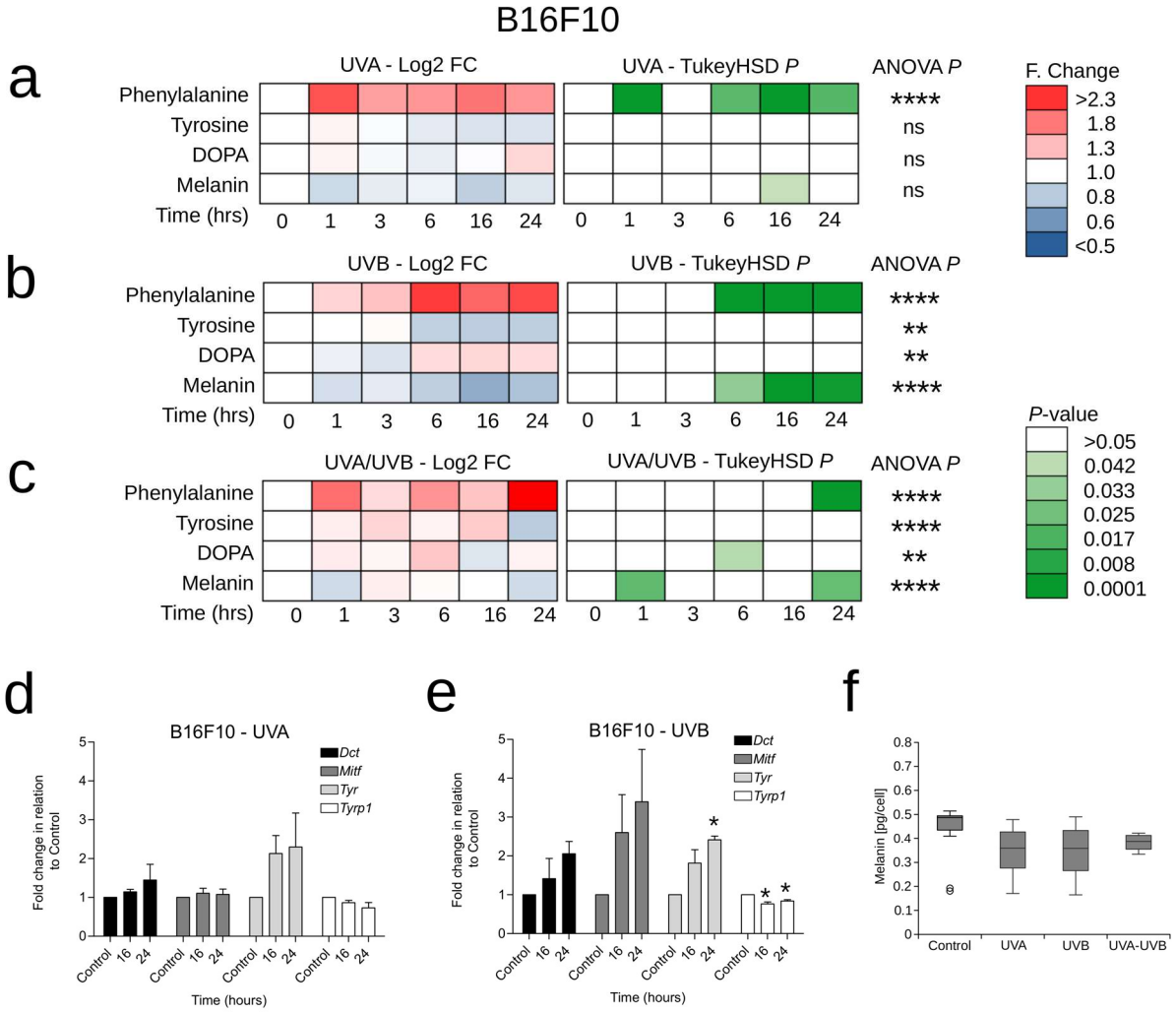
B16F10
a
UVA - Log2 FC
UVA - TukeyHSD P
ANOVA P
Phenylalanine
Tyrosine
DOPA
Melanin
Time (hrs)
0 1 3 6 16 24
****
ns
ns
ns
F. Change
>2.3
1.8
1.3
1.0
0.8
0.6
<0.5
b
UVB - Log2 FC
UVB - TukeyHSD P
ANOVA P
****
**
**
****
P-value
>0.05
0.042
0.033
0.025
0.017
0.008
0.0001
c
UVA/UVB - Log2 FC
UVA/UVB - TukeyHSD P
ANOVA P
****
****
**
****
d
B16F10 - UVA
Dct
Mitf
Tyr
Tyrp1
Fold change in relation to Control
Control 16 24
Time (hours)
e
B16F10 - UVB
f
Melanin [pg/cell]
Control
UVA
UVB
UVA-UVB

FIGURE 4:

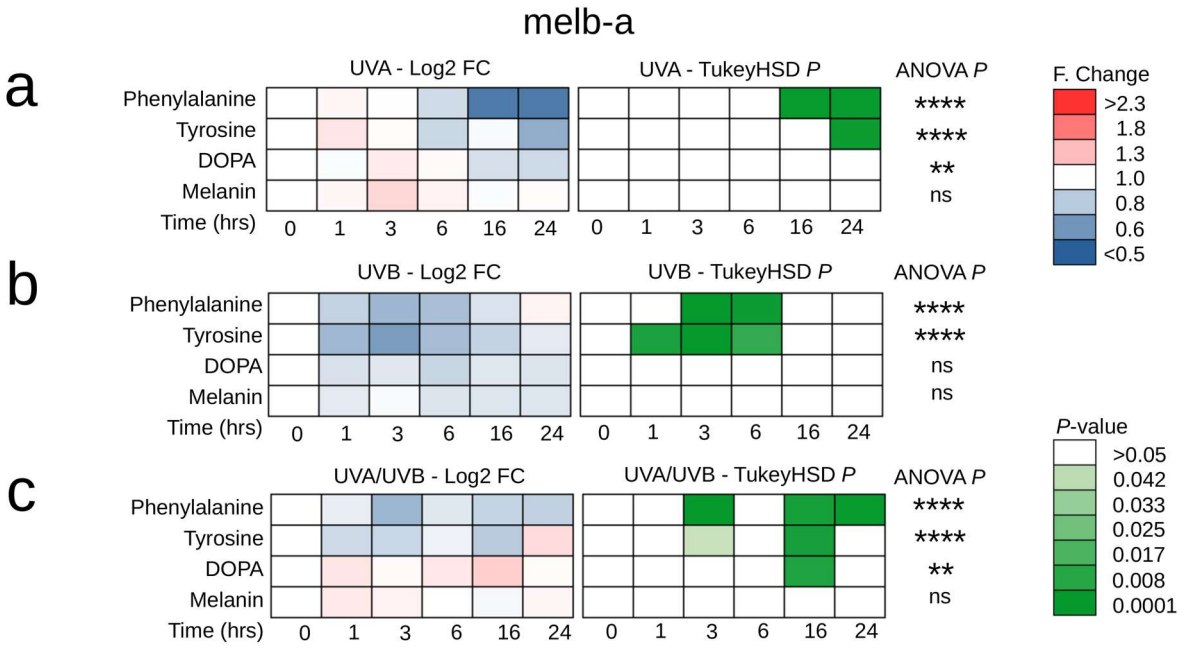
melb-a
a
UVA - Log2 FC
UVA - TukeyHSD P
ANOVA P
Phenylalanine
Tyrosine
DOPA
Melanin
Time (hrs)
0 1 3 6 16 24
****
****
**
ns
F. Change
>2.3
1.8
1.3
1.0
0.8
0.6
<0.5
b
UVB - Log2 FC
UVB - TukeyHSD P
ANOVA P
****
****
ns
ns
P-value
>0.05
0.042
0.033
0.025
0.017
0.008
0.0001
c
UVA/UVB - Log2 FC
UVA/UVB - TukeyHSD P
ANOVA P
****
****
**
ns

FIGURE 5:

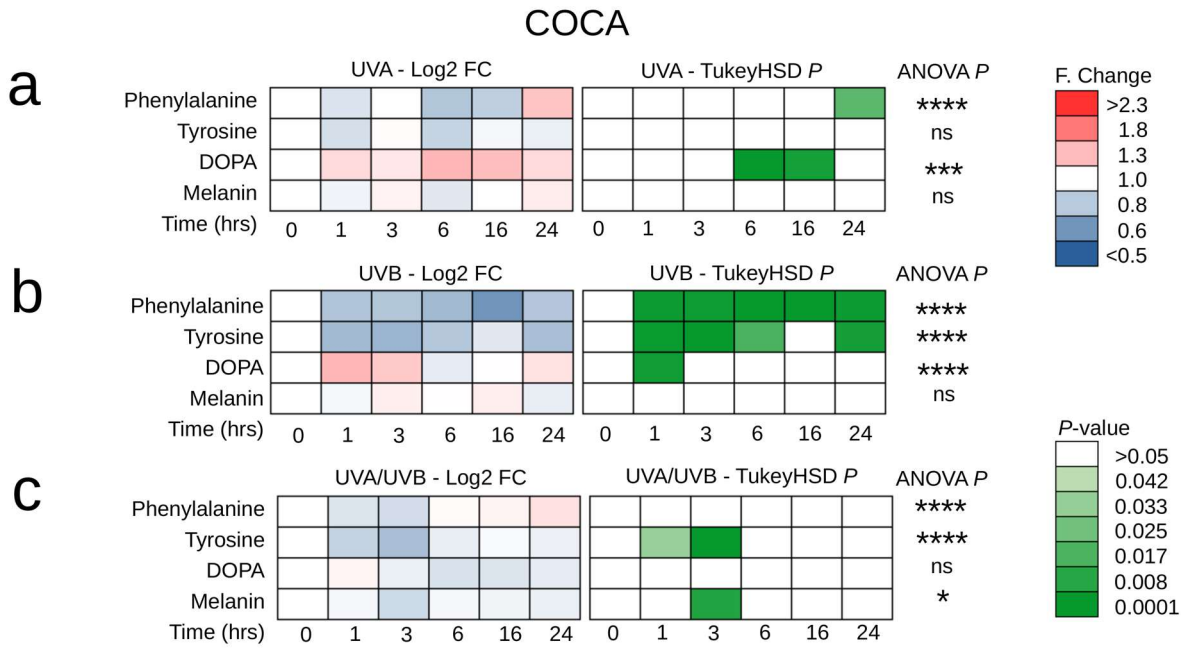
COCA
a
UVA - Log2 FC
UVA - TukeyHSD P
ANOVA P
Phenylalanine
Tyrosine
DOPA
Melanin
Time (hrs)
0 1 3 6 16 24
****
ns
***
ns
F. Change
>2.3
1.8
1.3
1.0
0.8
0.6
<0.5
b
UVB - Log2 FC
UVB - TukeyHSD P
ANOVA P
****
****
****
ns
c
UVA/UVB - Log2 FC
UVA/UVB - TukeyHSD P
ANOVA P
****
****
ns
*
P-value
>0.05
0.042
0.033
0.025
0.017
0.008
0.0001

FIGURE 6:

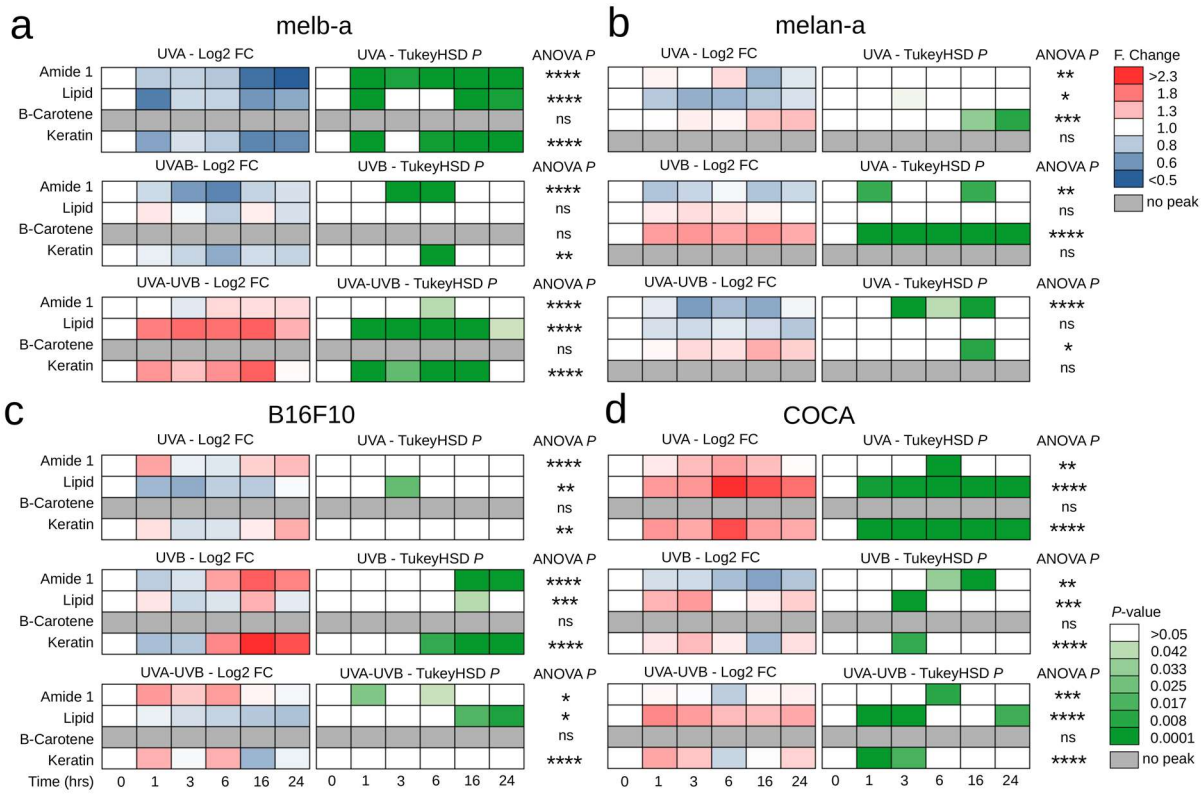
a
melb-a
b
melan-a
c
B16F10
d
COCA
UVA - Log2 FC
UVA - TukeyHSD P
ANOVA P
UVAB- Log2 FC
UVB - TukeyHSD P
UVB - Log2 FC
UVA-UVB - Log2 FC
UVA-UVB - TukeyHSD P
Amide 1
Lipid
B-Carotene
Keratin
Time (hrs)
0 1 3 6 16 24
F. Change
>2.3
1.8
1.3
1.0
0.8
0.6
<0.5
no peak
P-value
>0.05
0.042
0.033
0.025
0.017
0.008
0.0001
no peak